Nucl. Fusion **52** (2012) 089501 (1pp) doi:10.1088/0029-5515/52/8/089501

Corrigendum: Error field correction in DIII-D Ohmic plasmas with either handedness

2011 *Nucl. Fusion* **51** 023003

Jong-Kyu Park[1], **Michael J. Schaffer**[2], **Robert J. La Haye**[2], **Timothy J. Scoville**[2] **and Jonathan E. Menard**[1]

[1] Princeton Plasma Physics Laboratory, Princeton, NJ 08543, USA
[2] General Atomics, San Diego, CA 92186, USA

Received 26 April 2012, accepted for publication 25 May 2012
Published 13 June 2012
Online at stacks.iop.org/NF/52/089501

The expression for the overlap, equation (1) in the published paper (Park *et al* 2011 *Nucl. Fusion* **51** 023003), was incorrect and should be replaced by

$$\mathcal{C} \equiv \sqrt{\frac{\oint \mathrm{d}\varphi' [\oint \mathrm{d}a (\delta \vec{B}^x \cdot \hat{n}_b)(-\vartheta, \varphi' - \varphi)(\delta \vec{B}^x_d \cdot \hat{n}_b)(\vartheta, \varphi)]^2}{\oint \mathrm{d}a (\delta \vec{B}^x \cdot \hat{n}_b)^2 \oint \mathrm{d}a (\delta \vec{B}^x_d \cdot \hat{n}_b)^2}}. \tag{1}$$

We found that it would be worthwhile to add more descriptions. This is the root-mean-square integration over φ', after the convolution integral to ($\vartheta = 0, \varphi = \varphi'$) between the two distribution functions of magnetic field. The extra degree of freedom, only in the toroidal angle, is because the reference toroidal angle of the dominant field distribution $\delta \vec{B}_d(\vartheta, \varphi)$ can be arbitrary due to the toroidal symmetry in a tokamak. This expression becomes simply the dot product of the two normalized matrix vectors in the complex Fourier space, if one decomposes a magnetic field as

$$\sqrt{\mathcal{J}|\vec{\nabla}\psi|}(\delta \vec{B}^x \cdot \hat{n}_b)(\vartheta, \varphi) = \sum_{mn} \Phi_{mn} \mathrm{e}^{\mathrm{i}(m\vartheta - n\varphi)}. \tag{2}$$

Note the additional factor associated with the Jacobian of the surface area, $\mathcal{J}|\vec{\nabla}\psi|$, to have the surface area integral $\mathrm{d}a = \mathcal{J}|\vec{\nabla}\psi|\mathrm{d}\vartheta\,\mathrm{d}\varphi$ independent of coordinates. It is then straightforward to show equation (1) becomes the dot product between a given magnetic field $\vec{\Phi} = \{(m, n)|\Phi_{mn}\}$ and the dominant magnetic field $\vec{\Phi}_d = \{(m, n)|\Phi_{dmn}\}$ as

$$\mathcal{C} \equiv \frac{|\vec{\Phi} \cdot \vec{\Phi}_d|}{|\vec{\Phi}||\vec{\Phi}_d|}. \tag{3}$$

IOP Publishing and International Atomic Energy Agency Nuclear Fusion
Nucl. Fusion **51** (2011) 023003 (10pp) doi:10.1088/0029-5515/51/2/023003

Error field correction in DIII-D Ohmic plasmas with either handedness

Jong-Kyu Park[1], **Michael J. Schaffer**[2], **Robert J. La Haye**[2], **Timothy J. Scoville**[2] **and Jonathan E. Menard**[1]

[1] Princeton Plasma Physics Laboratory, Princeton, NJ 08543, USA
[2] General Atomics, San Diego, CA 92186, USA

Received 16 September 2010, accepted for publication 9 December 2010
Published 25 January 2011
Online at stacks.iop.org/NF/51/023003

Abstract
Error field correction results in DIII-D plasmas are presented in various configurations. In both left-handed and right-handed plasma configurations, where the intrinsic error fields become different due to the opposite helical twist (handedness) of the magnetic field, the optimal error correction currents and the toroidal phases of internal(I)-coils are empirically established. Applications of the Ideal Perturbed Equilibrium Code to these results demonstrate that the field component to be minimized is not the resonant component of the external field, but the total field including ideal plasma responses. Consistency between experiment and theory has been greatly improved along with the understanding of ideal plasma responses, but non-ideal plasma responses still need to be understood to achieve the reliable predictability in tokamak error field correction.

(Some figures in this article are in colour only in the electronic version)

1. Introduction

The sensitivity of toroidal plasmas to non-axisymmetric magnetic perturbations is well known in tokamak experiments. One of the most important consequences due to the non-axisymmetry is that magnetic islands can open and break magnetic surfaces, and eventually can lead to plasma disruption. The so-called *plasma locking* can occur with non-axisymmetry as small as $|\delta\vec{B}|/|\vec{B}| \approx 10^{-4}$, and thus the correction of such a small error field is an important issue in present tokamaks including ITER [1–8].

Plasma locking is the process by which the plasma rotation is stopped at the resonant surfaces in the presence of an external non-axisymmetric field. Plasma can shield the external perturbation and prevent magnetic islands from opening at the resonant surfaces, when the shielding currents can be sustained by plasma rotation and the electromagnetic torque by shielding currents can be compensated by the viscous torque by plasma rotation [9–11]. The balance between the electromagnetic torque and the viscous torque can break if the external magnetic perturbation and the electromagnetic torque is large enough. Then magnetic islands start to open and grow disruptively since electromagnetic torques become larger and viscous torques become smaller if islands become larger. This bifurcation process is called *error field penetration*, and the critical amplitude of the field can be defined as *error field threshold*. The error field threshold, however, is not easily defined, because the so-called intrinsic field error of a magnetic confinement device is usually the sum of more than one error source, so it has a complicated geometry and does not have an obvious unique general defining feature.

An empirical way to define an error field threshold is to use a known non-axisymmetric field source as a controllable test error field and add it in various ways to the system being studied. If the coil set produces a fixed poloidal field (PF) distribution, and if the field is decomposed into a single toroidal harmonic perturbation, the test error field can be defined by its current magnitude and toroidal phase. Then the error threshold can be defined by the locking current, e.g., by increasing the current until locking occurs while maintaining the same plasma conditions. The test error field in this paper is produced by I-coils in DIII-D, which are currently unique because they have two rows of off-midplane coil arrays. Thus, different PF distributions can be produced by changing the relative toroidal phase between upper and lower I-coil arrays. Then the error field threshold and the optimal correction should be defined for each relative toroidal phase.

Another fundamental way exists to change the field distribution given a set of coils, by reversing the relative direction between plasma current and toroidal field (TF). One can define right- and left-handed plasma states according to whether their magnetic field lines twist as right- or left-handed helices, respectively. In this paper, the right-handed plasma states are defined with plasma current and TF in the same toroidal direction. Similarly, the handedness of a helical Fourier harmonic is right-handed or left-handed depending on how its iso-phase lines (i.e. $m\vartheta - n\varphi = \text{const}$) twist. The

field distribution is observed differently for each configuration as described later.

The locking and the optimal correction currents can be defined for each relative toroidal phase between upper and lower I-coil arrays and for each left-handed and right-handed configuration. These empirical methods are useful in one device, however, one certainly needs to use a more physically relevant quantity that is involved in plasma locking dynamics, in order to give the predictability independent of the devices and their configurations. The error field has a 3D non-axisymmetric spatial distribution, and the mapping from a 3D distribution to a physical threshold is indeed the central issue in the error field study. When the error field sources are purely external to the plasma, one can specify a closed toroidal surface at which to specify the 3D spatial distribution of the error field. Since the external field $\delta\vec{B}^x$ obeys $\delta\vec{B}^x = -\vec{\nabla}\phi$ and $\nabla^2\phi = 0$, the field in space is completely determined by such a specification. Then one can decompose the field on the closed toroidal surface in the poloidal and the toroidal directions, and one can give the amplitudes of the field corresponding to the poloidal harmonics m and the toroidal harmonics n.

There have been many observations supporting the concept that in tokamaks the lowest toroidal harmonic perturbations, $n = 1$, are the most dangerous to plasma locking due to their deep penetrations and strong interactions with plasma [3–5, 8]. Therefore, one can focus on $n = 1$ in the error field study. The important poloidal harmonics in tokamak plasma locking depend more on the details of plasma profiles, but mostly the $m = 2$ harmonic perturbation at the $q = 2/1$ resonant surface appears to be associated with locking in typical tokamak operations. One, therefore, can use the $m = 2$ and $n = 1$ resonant component of magnetic field as the critical quantity to determine a locking property in tokamaks. Other components can contribute to plasma locking, by driving islands at other resonant surfaces or by braking rotation with the electromagnetic torques or neoclassical toroidal viscosity (NTV) [12–14], but are considered subdominant in this paper. Whether or not the choice of the critical field component is valid for locking dynamics should be addressed by scaling with kinetic parameters.

The determination of the $m = 2$ and $n = 1$ resonant field requires the calculation of 3D tokamak equilibria. The previous studies often used the *vacuum superposition* approximations, since vacuum calculations of the field from the currents in the external sources δB^x are used to calculate resonant component $\delta B^x_{mn} \equiv (\delta\vec{B}^x \cdot \hat{n})_{mn}$. However, the approximation by the vacuum superposition is valid only in limited conditions, and therefore requires empirical coupling coefficients between other components to explain experiments as performed by three-mode coupling methods [3, 4]. The two main improvements can be made upon the previous approximations. (1) The resonant component, either without or with plasma, should be calculated based on the flux being independent of the choice of magnetic coordinates [15]. This includes fundamental geometric coupling effects. (2) The resonant component should be calculated with plasma responses since it can be largely different from the external resonant component. This paper uses (1) the corrected external resonant field δB^x_{21} and (2) the total resonant field δB_{21} to include plasma responses.

Note that the total resonant field is suppressed by shielding currents before the onset of locking, and would drive islands if shielding currents are all dissipated [6]. The external resonant field is originally used to approximate the total resonant field [10], but the conditions where this approximation actually holds are fairly limited; the resonant surface must be located in the edge so that most of the plasma pressures and currents are located inside the resonant surface. Also, the plasma must be close to a circular cylindrical geometry so that poloidal intermodal coupling can be ignored. For a perfect circular cylinder without pressures, and without currents outside the resonant surface, the external resonant field and the actual resonant field driving islands can be identical [16]. However, in tokamaks, perturbed plasma currents are strong enough to fundamentally change the resonant field from the vacuum approximation.

The importance of plasma response, which is a part of the total resonant field driving islands, has been demonstrated in error field problems by the applications of the Ideal Perturbed Equilibrium Code (IPEC) [6, 17]. This paper presents further sound evidence based on the dedicated error field correction experiments in DIII-D, by utilizing its unique capability to change the field distributions. The paper is organized as follows. Section 2 describes details of the intrinsic error field in DIII-D and of optimal corrections by I-coils in left-handed and right-handed configurations. Physics analysis is provided in section 3, using both the total resonant field in IPEC and the external resonant field in vacuum superposition method in order to explain the error field threshold found in various configurations. Section 4 discusses the essential feature of the dominant field distribution.

2. Intrinsic error fields and I-coil corrections

2.1. Intrinsic error fields in DIII-D

This section provides a history for the key features of the intrinsic error field and correction in DIII-D since this paper covers experiments performed in different years. Improvements for the unknown sources of intrinsic error field and correction have been empirically achieved over many years, but understanding of the actual 3D plasma equilibrium including plasma responses was ultimately required to improve the consistency between experiment and theory.

The DIII-D tokamak [18] was significantly affected during its first years of operation by $n = 1$ locked plasmas, especially at low plasma densities. After it was discovered in 1990 that the so-called $n = 1$ *coil* (a single circular coil installed to study effects of deliberate non-axisymmetric magnetic perturbations) could also partially reduce plasma locking, it was realized that at least some lockings were caused by imperfect axisymmetry of the tokamak magnetic field [19]. Motivated by the need to better understand and control locking, the first direct measurements of the DIII-D intrinsic error field were made in 1990 [20]. An array of magnetic field detection coils was temporarily assembled inside the open vacuum vessel and carefully aligned with the magnetic field of the DIII-D toroidal magnetic field coils. The data indicated that the PF coils (called F-coils at DIII-D) were variously shifted and tilted relative to the TF. The F-coils are identified in figure 1. In the

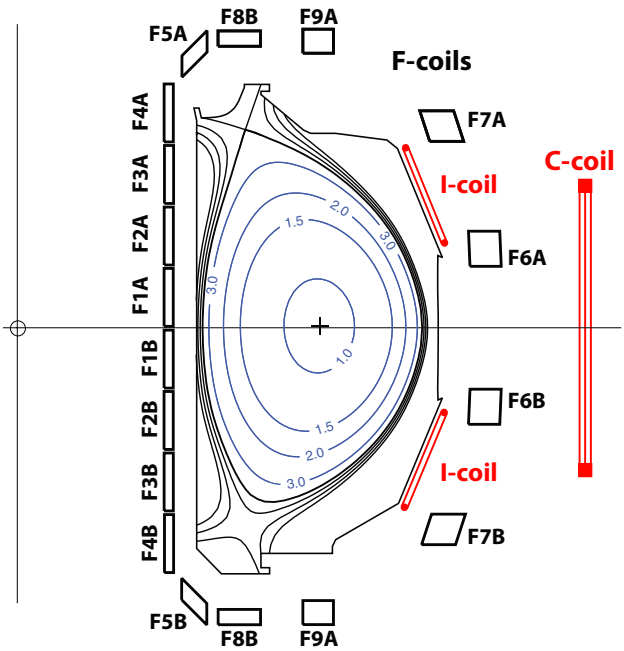

Figure 1. Cross section of DIII-D in the year 2006, illustrating locations of the PF F-coils, one C-coil and two I-coils, with respect to a typical Ohmic plasma ($q_{95} = 3.3$, $B_{T0} = 1.0T$, $\beta_N = 0.5$) used for the error field and locking experiments.

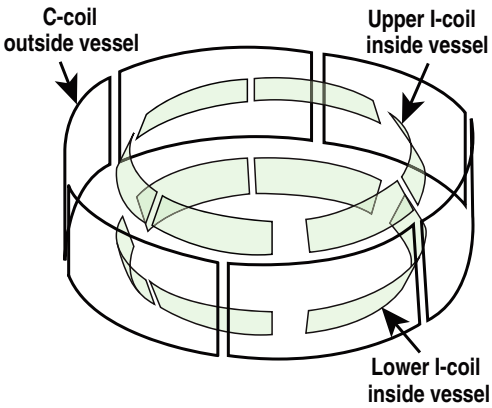

Figure 2. Illustration of C-coils and I-coils in DIII-D.

worst case, coil F7A, one of the four coils on the low-field side of the plasma used to apply vertical field, was reported to have shifted horizontally about 19 mm from the TF magnetic centre, and coils F5A, F8A and F9A were tilted 14 $\sim$ 16 mm from the plane of the TF. These are $\sim$2 times larger than their specified allowable placement errors. The other significant known error sources were two large TF-coil current feeds, whose error fields were calculated from their known geometries. One of the feeds became temporarily accessible in 2005, and it was rebuilt for low error field. This paper includes data from experiments in 2004 with the larger current feed error, as well as experiments since 2006 with a smaller error.

Having discovered the geometry of the DIII-D PF error, a flexible coil array was designed for error correction (the *C-coils*) and was installed in 1994. It consists of six approximately rectangular coils, spaced uniformly around the tokamak outside the TF coils, and centred vertically about the tokamak midplane. The array geometry is illustrated in [4] and here in figure 2. The C-coils are connected to three power supplies to generate an $n = 1$ magnetic field of arbitrary toroidal phase in the plasma volume while keeping the $n = 3$ harmonic zero. The optimal amplitudes and toroidal phases for the best locked plasma avoidance in low-density, low-β, Ohmically-heated plasmas that are reproducibly sensitive to locking were found by a fit to the data from dedicated locking experiments. Error correction by the combined $n = 1$ coil and C-coils was better than by either one alone [4].

An array of 12 identical internal coils (*I-coils*) was installed in 2003, initially for active feedback stabilization of RWMs [22]. The array consists of six coils almost equally spaced in each of the two rows around the torus, an upper row above the tokamak outer midplane and a mirror lower row below it (see figure 2). It was quickly determined that the I-coils were also good error correction coils. For the case of $n = 1$ current distributions in both rows, the I-coil array allows three degrees of freedom. First, the toroidal phasing, $\Delta\phi = \phi_{\text{lower}} - \phi_{\text{upper}}$, is the difference between the lower and upper $n = 1$ current harmonic phases. Second, the toroidal phase, $\phi_0 = (\phi_{\text{lower}} + \phi_{\text{upper}})/2$, is the average phase of the two current harmonics. This phase is also, within a few degrees, the toroidal phase of the $n = 1$ Fourier harmonic of $\delta B^x \cdot \hat{n}$ just inside the last closed flux surface. The third independent variable is the magnitude of the Fourier coefficient (peak amplitude) of the upper and lower $n = 1$ currents, I_{peak}, which were equal in the experiments reported here. At DIII-D each I-coil is paired with the coil diametrically opposite, and the two are connected electrically in series for opposite current directions. Then, each lower pair is connected electrically in series with the upper pair that is the desired phasing $\Delta\phi$ away toroidally. A set of four connected coils is called a 'quartet', and each quartet is powered by one of the three independent bipolar power supplies. As with the C-coils, the power supplies are programmed to produce an $n = 1$ harmonic with no $n = 3$. However, even the improved correction using I-coils did not obey the expected outcome, the low rational resonant Fourier harmonics of the measured external intrinsic error and correction fields would be approximately equal in magnitude and 180° out of phase. Instead, there appeared to be a still unknown large intrinsic error source. Meanwhile, the resulting empirical error correction algorithm was subsequently applied routinely and beneficially to most DIII-D discharges.

The accumulating uncertainty of the true DIII-D intrinsic error motivated a new, thorough, direct measurement campaign to find all significant error sources. It improved upon [20] by referencing the magnetic measurements to absolute benchmarks rather than to the TF [23]. The new results most relevant to this paper were (1) the mutual misalignments between the PF and TF coils are moderately smaller than reported in [20], but they are still larger than design specifications; (2) the TF coil is shifted horizontally by 4.5 mm from its specified position and tilted 1.05 mrad from vertical alignment, both out of specification; (3) despite extensive searching, no other new large errors were discovered. Figure 3 shows the recalculated spectrum of the intrinsic error field before 2005 (with the larger TF feed error) based on the new measurements, and figure 4 shows the spectrum of the intrinsic error field after 2005 (with the smaller TF feed error). Note in

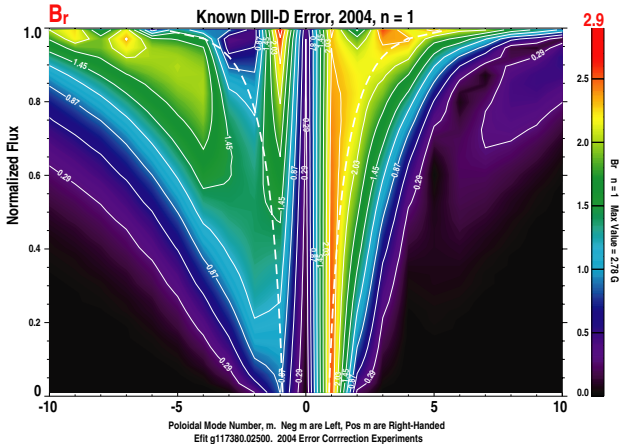

Figure 3. The spectrum of DIII-D intrinsic error fields before 2005. It is calculated using the external field normal to flux surfaces (SURFMN code [21]). One can see the asymmetry between the positive and the negative poloidal harmonics m, which are resonant with the right-handed and the left-handed configuration, respectively. The curve $m = \pm nq$ for $n = 1$ is shown by white dashed lines.

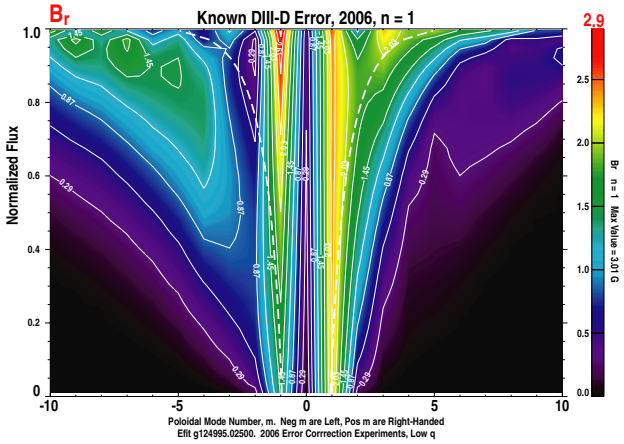

Figure 4. The spectrum of DIII-D intrinsic error fields, as in figure 3, but after the large TF feed error is removed in 2005. This is the valid error spectrum up to present. One can see the field amplitudes are reduced in general, compared with figure 3.

figure 4 that the near absence of the $m = -2$ harmonic in the DIII-D external intrinsic error field at the left-handed $q = 2$ surface at $\psi_N = 0.78$; in other words, $\delta B^x_{21} \approx 0$. If δB^x_{21} were the important variables for locking, then the present DIII-D intrinsic error field should be nearly optimum against locking with no further error correction, contrary to the experiment.

Empirical error correction at DIII-D appears to function by bringing the combined external and plasma-generated PFs into better alignment with the TF, so the magnetic consequences of findings (1) and (2) were not fundamentally changed by the new information. However, the vacuum vessel is correctly positioned, and DIII-D diagnostics are aligned with vessel benchmarks. This means that if the error-corrected plasma aligns with the TF, then the plasma is eccentric with respect to the vessel and the diagnostic coordinate system. Ultimately it was necessary to understand the actual 3D plasma equilibrium shape in the presence of intrinsic errors and imperfect error correction.

It has long been known that the error field threshold is proportional to the locking density threshold [2–6, 8]. For a steady magnetic perturbation (intrinsic error field plus the known field of a selected I-coil and/or C-coil current configuration), the density threshold can be found by allowing the plasma density to decay slowly until a locked mode is detected. Alternatively, one may find a locking current threshold at a fixed plasma density and toroidal phase angle by slowly ramping the magnitude of the coil current distribution until a locked mode is detected. These methods were used to study the locking threshold in DIII-D [2], COMPASS-D and JET [3, 24] and now become the conventional method in many tokamaks, such as NSTX [8], CMOD [5] and MAST [7]. Either way, the effective error field locking threshold is expressible experimentally as the number $(I_{\rm peak}/n_{\rm e})$ which varies with error field geometry but is nearly a constant for any particular error field. Then the optimal toroidal phase for the correction geometry being tested corresponds to the maximum $I_{\rm peak}/n_{\rm e}$. The larger critical currents imply that the combination provides the field distributions against the intrinsic error field distributions, indicating the combination is close to optimal toroidal phase. When the spectrum of the test error field is fixed except for the toroidal phase, the amplitude and phase of optimal correction can be determined by investigating the different amplitudes at each phase and its resulting non-axisymmetry [24]. The difference for DIII-D is that various spectra of the applied field are possible by varying the toroidal phasing $\Delta\phi$ of I-coils and so the optimal amplitude and phase are also different. Thus, there is one more degree of freedom for the toroidal phase in DIII-D, due to one more row of coils, which enables us to investigate effects by different spectra of the test error field.

The locking threshold in low-density diverted Ohmic plasmas is very reproducible in a given tokamak, and such plasmas have been used for inter machine comparison [3, 24]. At DIII-D the TF direction is normally set so that the ion grad B drift is downwards, which gives the lowest heating power threshold for transition to H-mode confinement for lower single-null diverted plasmas. However, Ohmic plasmas at low densities in DIII-D often make a transition to H-mode part way through a discharge, which makes an uncontrolled change in plasma locking properties. Therefore, the locking experiments were conducted with slightly upper single-null diverted plasmas in order to remain in L-mode with the normal DIII-D TF direction, and then the plasma is pumped by the DIII-D upper cryopump.

2.2. I-coil corrections in left-handed plasmas

Optimal corrections for left-handed plasmas are practically more important for DIII-D, since most plasma operations are performed in left-handed configurations. Locking experiments in left-handed plasmas were conducted at fixed $n_{\rm e}$ with many different spectra in 2004 (i.e. with the larger TF feed error) for six phase differences $\Delta\phi$, each tested at four different toroidal phase orientations ϕ_0. For each $\Delta\phi$, the optimal correction current amplitude and ϕ_0 were found using the standard technique [24] by a *polar map* of the applied current vectors. Similar experiments were performed after 2006 (i.e. with the smaller TF feed error), but with only limited cases for $\Delta\phi$.

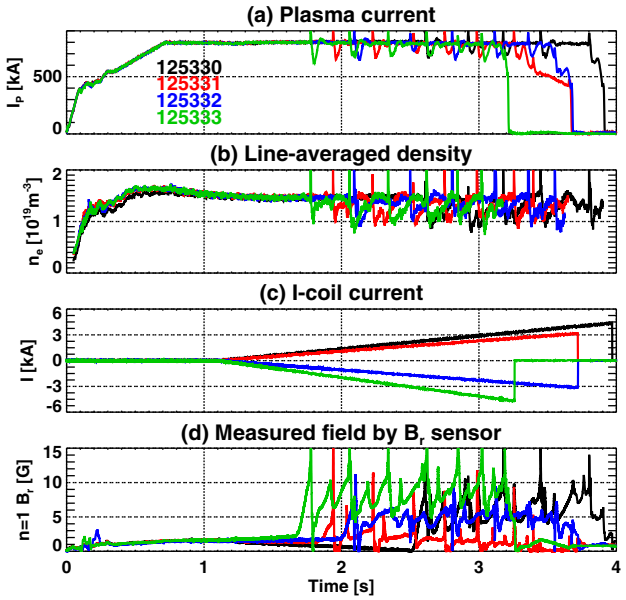

Figure 5. Locking experiments with I-coil phasing $\Delta\phi = 240^\circ$ and toroidal phases $\phi_0 = 60^\circ, 150^\circ, 240^\circ, 330^\circ$ for the left-handed plasma configuration. (*a*) Plasma currents, (*b*) densities are maintained identical and (*c*) different I-coil currents produce (*d*) locking (measured by B_r sensors) at different thresholds.

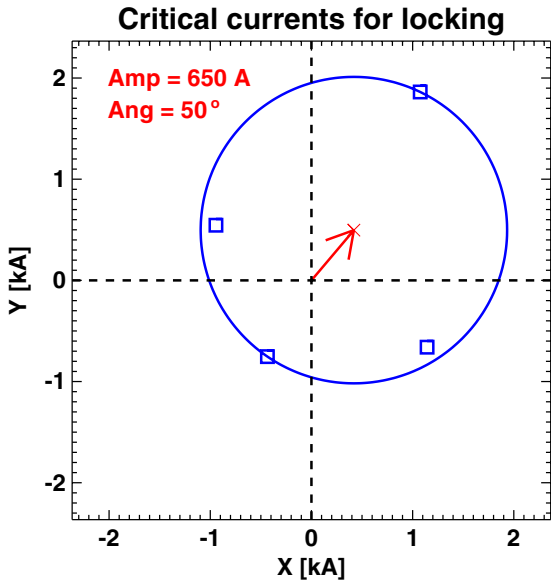

Figure 6. Polar map showing coil current locking threshold amplitudes and toroidal phases ϕ_0 for the four left-handed shots of figure 5. A shifted circle is fitted to the four data points. The circle radius is the $n = 1$ current required in the I-coil set using $\Delta\phi = 240^\circ$ phasing geometry to lock these test plasmas. The coil centre and arrow mark the optimal $n = 1$ correction current, 650 A with $\phi_0 = 50^\circ$ phase.

Figure 5 shows the comparisons of four 2006 locking shots, using I-coil phasing $\Delta\phi = 240^\circ$ and the toroidal phases $\phi_0 = 60^\circ, 150^\circ, 240^\circ, 330^\circ$. One can see the different I-coil currents from the traces (*c*), and the different time and critical currents of locking from the traces (*d*), while the plasma parameters are kept in the same values as can be seen from (*a*) the plasma currents and (*b*) the plasma densities. The optimal correcting toroidal phase can be determined using a polar map and representing the amplitudes and toroidal phases of the critical currents of locking. Figure 6 shows the polar map of the amplitudes and the phases of the I-coil current distributions at the time of locking. The non-axisymmetry indicates the existence of intrinsic error fields. The effective I-coil current amplitude and phase are determined by finding the centre of the shifted circle fitted to the data. The coil equivalent error of intrinsic error field in this configuration is equal and opposite to this optimal correction. Note that although the circle can be found with just three toroidal phases, one more toroidal phase is used in our studies to verify data consistency and to estimate experimental errors.

This method is indeed very useful for finding optimal corrections as one can see from figure 7, where the standard test plasma with uncorrected intrinsic error has critical locking density $0.85 \times 10^{19}\,\mathrm{m}^{-3}$. However, with the correction shown in the polar map, figure 6, one can see the improved performance and the reduced locking density, $0.38 \times 10^{19}\,\mathrm{m}^{-3}$, in shot 125335.

2.3. Optimal toroidal phasing

The optimal toroidal phasing $\Delta\phi$ for I-coil coupling to error correction can also be determined by seeking the smallest I-coil peak current, that is, the smallest optimal current vector in the polar map. The smaller I-coil peak current obviously

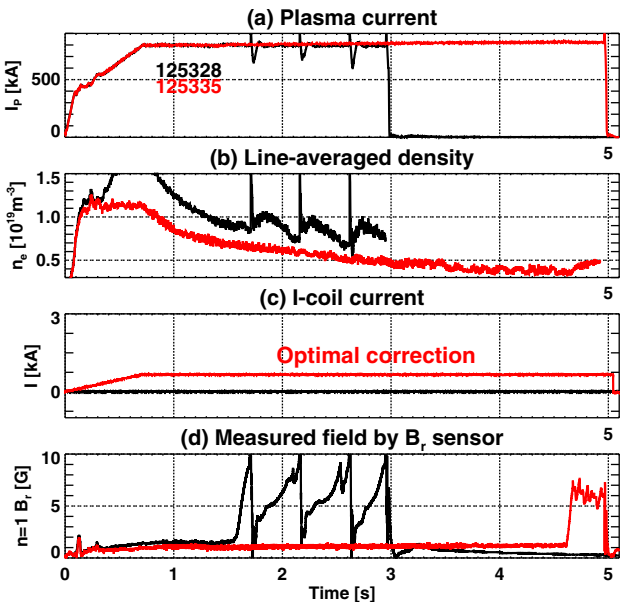

Figure 7. Locking experiments using the optimal correction found by figure 6 for the left-handed plasmas. The correction significantly reduces the critical locking density (red) compared with no corrections (black).

implies less power and thus a more efficient configuration of correction coils for compensating the intrinsic error.

A set of experiments in 2004 searched for the optimal toroidal phasing to correct the intrinsic error, using six different $\Delta\phi = 0^\circ, 60^\circ, 120^\circ, 180^\circ, 240^\circ, 330^\circ$. In the first set of experiments, the density was maintained at the level of $2.3 \times 10^{19}\,\mathrm{m}^{-3}$. One problem found in those experiments was that this density was too high and the plasma was never locked when

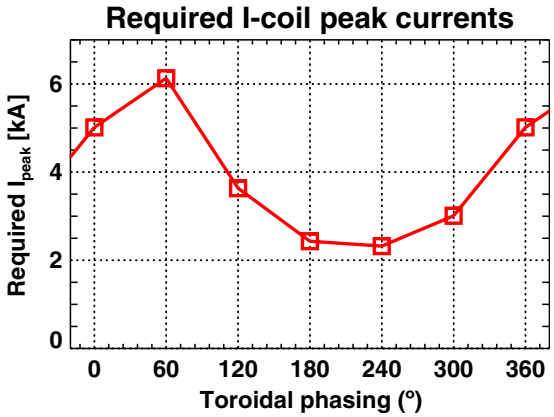

Figure 8. Required I-coil $n = 1$ peak currents for optimal corrections versus different toroidal phasings, for the pre-2005 intrinsic error. One can see the optimal phasing at $\Delta\phi = 240^\circ$ and the worst phasing at $\Delta\phi = 60^\circ$.

$\Delta\phi$ was too unfavourable, such as $\Delta\phi = 0^\circ \sim 120^\circ$, even with the highest currents possible in I-coils. The error field locking threshold is known to be approximately proportional to the plasma density at locking, if the distribution of the applied field is kept identical, as found in many other experiments [2–6, 8]. Therefore, the experiments were revisited later at a lower density level, $1.5 \times 10^{19}\,\mathrm{m}^{-3}$, for those unfavourable phasing cases. Combining the two sets of experiments based on the linear dependence of the error field threshold to locking density, one can compare I_{peak} for optimal correction at $n_{\mathrm{e}} = 1.5 \times 10^{19}\,\mathrm{m}^{-3}$, among each toroidal phasing, as shown in figure 8. The smallest I_{peak} can be found at $\Delta\phi = 240^\circ$, which means that one can correct the error field most efficiently with $\Delta\phi = 240^\circ$.

The optimal toroidal phasing $\Delta\phi = 240^\circ$ that one can see from figure 8 is the result in 2004, so one may speculate that it may not be optimal anymore due to the different intrinsic errors. However, the total resonant field δB_{21} by I-coils is independent of intrinsic error among each toroidal phasing, and thus different intrinsic errors would not change the relative amplitudes of compensating currents in each toroidal phasing. This would not be true if other components become important. If one assumes other components to be subdominant and uses perturbation methods, as in this paper, one can still use $\Delta\phi = 240^\circ$ as the optimal toroidal phasing for the new error fields. This is why the I-coil correction experiments in 2006 (section 2.1) used only the $\Delta\phi = 240^\circ$ phasing to find the optimal correction. However, the optimal toroidal phasing is dependent on plasma configurations and parameters, such as q_{95}.

2.4. I-coil corrections in right-handed plasmas

Right-handed plasmas are made by reversing either B_{T} or I_{p} from its standard direction, but not both. The right-handed plasma in the Ohmic DIII-D experiments reported here had reversed B_{T}. There is no demarcation in magnetic geometry between the left-handed and the right-handed case in tokamaks. However, the fundamental difference between the left-handed and the right-handed cases can occur in the presence of 3D non-axisymmetry. The two configurations have

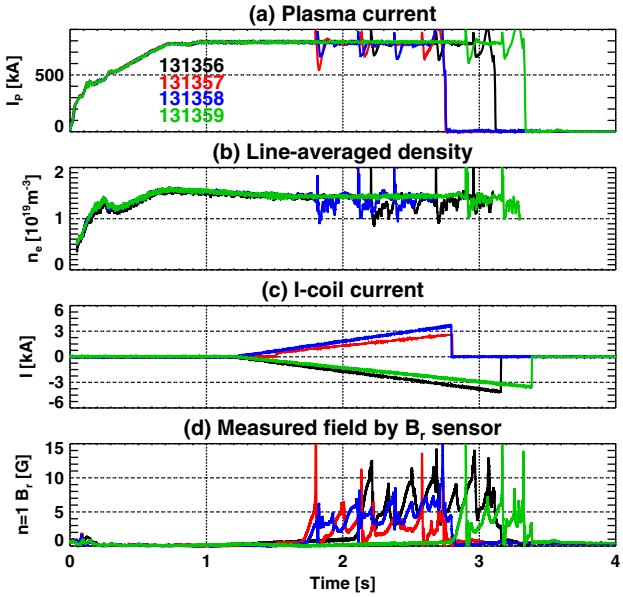

Figure 9. Locking experiments with I-coil phasing $\Delta\phi = 120^\circ$ and toroidal phases $\phi_0 = 60^\circ, 150^\circ, 240^\circ, 330^\circ$ for the right-handed configurations. (*a*) Plasma currents, (*b*) densities are kept identical and (*c*) different I-coil currents produce (*d*) locking (measured by B_r sensors) at different thresholds.

the opposite favourable pitch and thus respond to different resonant components from the same intrinsic error field sources. The experiments for DIII-D I-coil corrections in right-handed plasmas were conducted to confirm the theory and the source of intrinsic errors, as well as to reduce locking that interfered with right-handed experiments at low densities.

DIII-D experiments on error correction of right-handed configurations were performed with toroidal phasing $\Delta\phi = 180^\circ$ in 2007. This I-coil phasing was chosen because calculations showed that its $n = 1$ external field most efficiently cancelled the $n = 1$ external field resonant harmonics of right-handed DIII-D configurations. This is before the new IPEC results were well known at DIII-D. However, experiment showed $\Delta\phi = 180^\circ$ to be only weakly effective at reducing the critical locking density. Then, in 2008 with insight from successful IPEC interpretation of some left-handed configurations, right-handed error correction experiments were repeated with $\Delta\phi = 120^\circ$, which is the optimum I-coil phasing to couple to the right-handed dominant mode. This is because again the optimal toroidal phasing is nearly independent of the intrinsic error fields, and it is a property of the plasma equilibrium and its helical magnetic field pitch. The helical pitch is changed only by the toroidal direction in the right-handed configuration, so one can easily figure out the optimal toroidal phasing for the right-handed plasmas should be $\Delta\phi = 360^\circ - 240^\circ = 120^\circ$, i.e. the 120° I-coil phasing in right-handed plasmas is equivalent to 240° in left-handed plasmas.

Figure 9 shows the comparisons of locking experiments using I-coil phasing $\Delta\phi = 120^\circ$ and toroidal phases $\phi_0 = 60^\circ, 150^\circ, 240^\circ, 330^\circ$ in the right-handed configurations. As in figure 5, one can see the different I-coil currents from the trace (*c*), and the different time and critical currents of locking (*d*) for the same plasma parameters such as (*a*) the

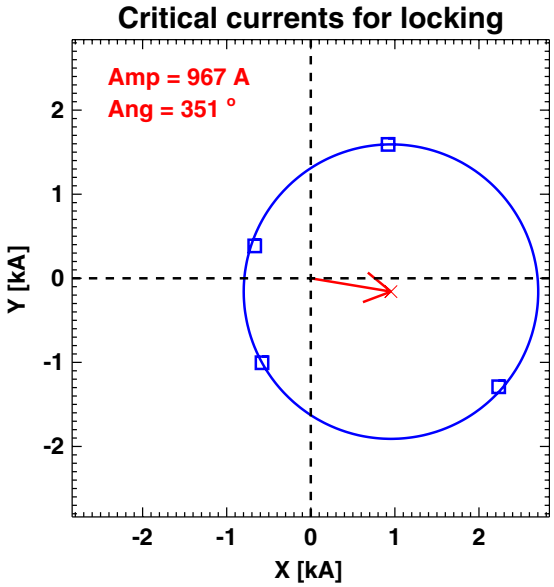

Figure 10. Polar map showing coil current locking threshold amplitudes and toroidal phases ϕ_0 for the four right-handed shots of figure 9. A shifted circle is fitted to the four data points. The circle radius is the $n = 1$ current required in the I-coil set using $\Delta\phi = 120°$ phasing geometry to lock these test plasmas. The coil centre and arrow mark the optimal $n = 1$ correction current, 967 A with $\phi_0 = 351°$ phase.

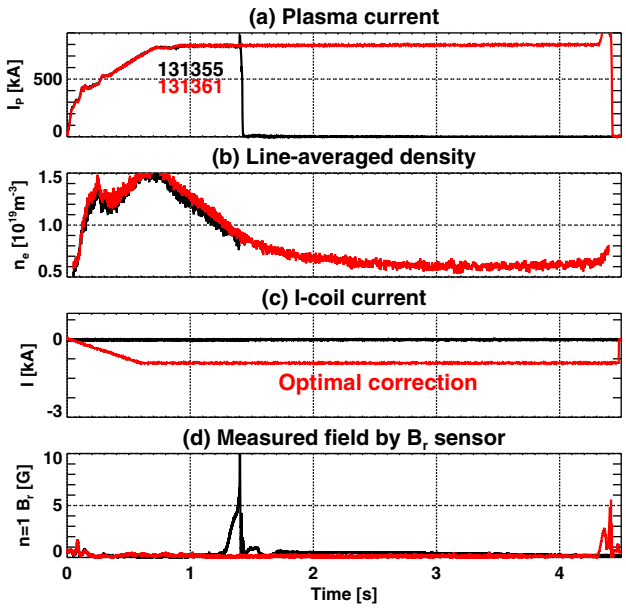

Figure 11. Locking experiments using the optimal 120° phasing correction found in figure 10 for the right-handed plasmas. The correction significantly reduces the critical locking density (red) compared with no corrections (black).

plasma currents and (*b*) the plasma densities. Using the optimal currents that can be found by the polar map, figure 10, the critical density could be reduced down to 0.53×10^{19} m^{-3} as can be seen from figure 11.

3. Theory—total and external resonant fields driving islands

The optimal corrections in the left-handed and right-handed plasmas can be used to mitigate the error field effects in plasma operations. The results were found empirically, but were not successfully understood theoretically when vacuum approximations calculated from 'known' coil irregularities were used. As has been demonstrated in IPEC in recent years, the effect of plasma response cannot be ignored even in Ohmic plasmas.

IPEC calculates the resonant field driving magnetic islands, which is suppressed by shielding currents before the onset of islands and locking. It can be called *total resonant field* since it is the result calculating $\delta\vec{B}^x + \delta\vec{B}^p$ including the field by plasma response currents $\delta\vec{B}^p$, and the resonant field by vacuum approximations will be called *external resonant field* since it includes only the field $\delta\vec{B}^x$ from external currents. If plasma is force-free, circular–cylindrical, and also current-free outside a resonant surface, the resonant field by vacuum approximation and IPEC give an identical value. However, vacuum methods cannot approximate tokamak plasmas in general. In this section, more supporting examples will be illustrated based on our experiments.

Figure 12 shows that the (*a*) 2/1 total resonant fields calculated by IPEC for locking experiments with $n_e \sim 2.3 \times 10^{19}$ m^{-3}. The locking value of the resonant field should be independent of ϕ_0 in identical plasmas if all the external magnetic perturbations (intrinsic + I-coils) are included, as can be seen with locking cases with a favourable phasing $\Delta\phi = 300°$. The unfavourable phasing $\Delta\phi = 60°$ did not make locking at any ϕ_0 and one can see the consistent results; the 2/1 total resonant fields are not sufficient to reach the critical value, even if the available maximum currents (∼6 kA) in I-coils are used in this unfavourable phasing. In contrast, one can see the inconsistency presented by the (*b*) 2/1 external resonant fields. The external resonant fields are small for locking cases and are large for non-locking cases, which is opposite to observations. Also, one can see the critical amplitude for locking cases has a large standard deviation and varies by 100% between $\phi_0 = 60°$ and 240° for nearly the same plasma conditions. These observations indicate the inaccuracies of vacuum approximations in error field problems. Note that strong plasma responses, for the $n = 1$ applied field, that are evident in our studies, may not be true for higher n, and remains to be investigated in a future study.

The error field correction experiments in right-handed cases also showed that the total resonant field describes locking far better than the external resonant field. Again the resonant field driving magnetic islands is expected to be independent of ϕ_0 since all other plasma parameters including plasma density are kept constant. One can see figure 13 shows, similar locking values by the total resonant fields, but the locking values by the external resonant fields change largely beyond a meaningful fit as can be seen by large standard deviations.

Figure 13 also illustrates that the critical total resonant field can be varied by plasma parameters other than the plasma density. One can see the critical amplitudes by the total resonant fields are different when the TF strength B_{T0} is changed. This negative B_{T0} scaling has also been reported in other experiments [5], consistently with present examples. However, parameters other than the plasma density do not vary much in DIII-D Ohmic plasmas that are being covered in this

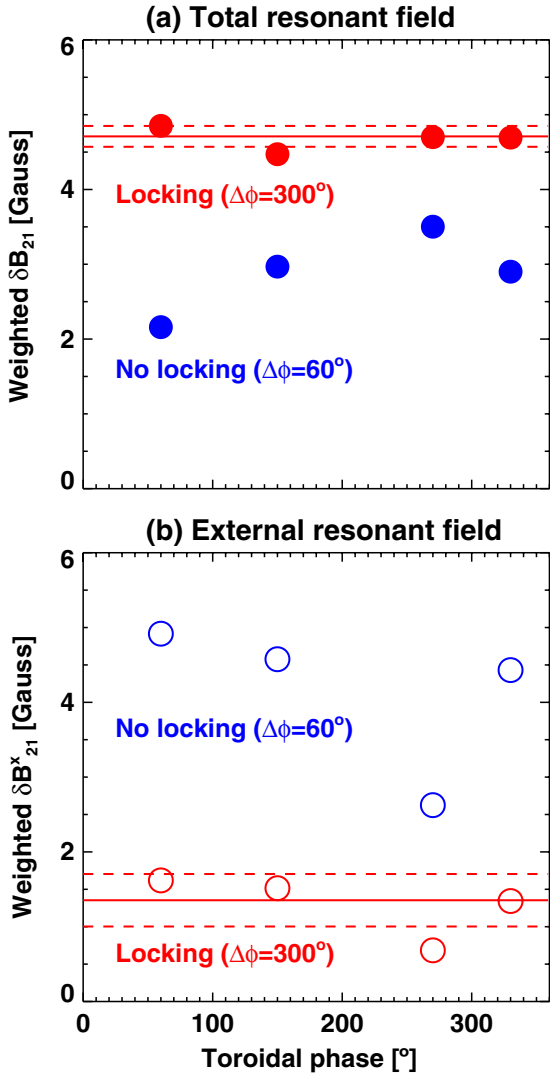

Figure 12. Comparisons between (*a*) the total resonant fields at $q = 2$ and (*b*) the external resonant fields at $q = 2$, for the locking cases by the favourable phasing $\Delta\phi = 300°$ (red) and the cases with no locking by the unfavourable phasing $\Delta\phi = 60°$ (blue), in the left-handed configurations. The solid line is the average for locking cases and the dashed line shows the standard deviation. The total resonant fields are far more consistent: locking vales are higher than non-locking cases and are all in similar amplitudes (red).

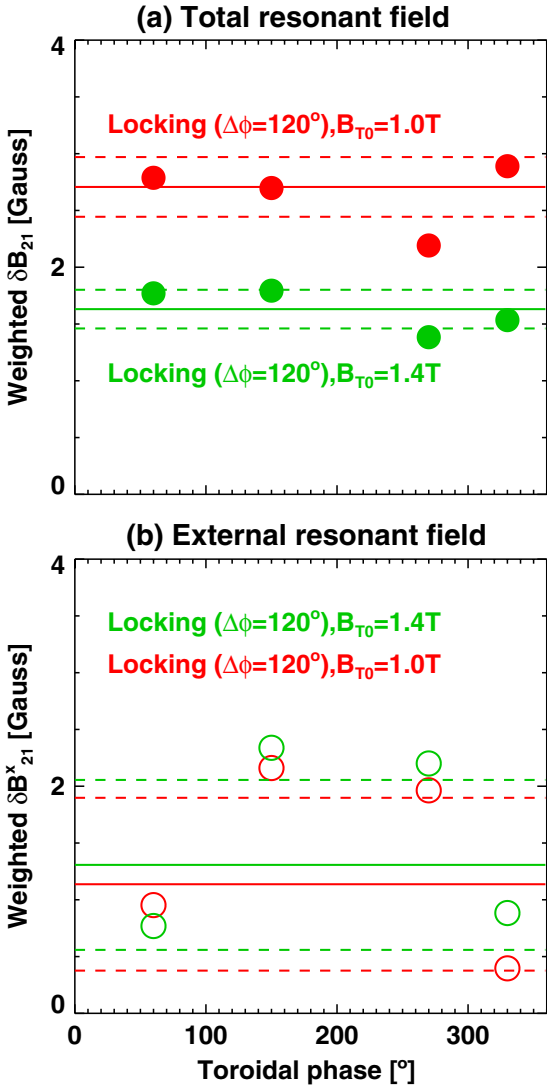

Figure 13. Comparisons between (*a*) the total resonant fields at $q = 2$ and (*b*) the external resonant fields at $q = 2$, for the locking cases by the favourable phasing $\Delta\phi = 120°$ (red), in the right-handed configurations. The solid line is the average for locking cases and the dashed line shows the standard deviation. The total resonant fields are more consistent: locking values are all in similar amplitudes. The external resonant fields change largely beyond a meaningful fit as can be seen by large standard deviations. Comparisons for the higher TF are also shown (green), indicating the negative scaling when the total resonant field is used.

paper, and so here only the density correlation with the resonant field is considered.

The various error field correction experiments and their locking data are summarized in figures 14 and 15. Figures include locking data presented previously in [6] (red), and error field correction data for the left-handed (green) and right-handed (blue, marked with □ for $B_{T0} = 1.4$ T) plasmas introduced in this paper. One can see the apparent linear density correlation between the critical field and the density in figure 15 when the IPEC total resonant fields δB_{21} are used. On the other hand, figure 14 shows the poor correlation when the external resonant fields δB^x_{21} are used. In fact it is very difficult to draw any conclusion from the results. For instance, the error field correction experiments with the high density $n_e \sim 2.0 \sim 2.3 \times 10^{19}\,\mathrm{m}^{-3}$ give all possible values below the critical amplitude δB^x_{21} as one can see.

Although figures 14 and 15 show a far better representation for the error field and locking when δB_{21} is used rather than δB^x_{21}, but a significant data scatter also exists with δB_{21}. It can come from other sources of intrinsic errors, or other parametric dependences, which perhaps may improve the correlation in scaling. A detailed discussion on locking scaling will be saved for future work since it should be based on a wider range of parameters including other tokamaks.

A more important issue is the offset of the linear correlation towards $\delta B_{21} \to 0$. The offset indicates that locking still occurs even if the resonant field component is completely removed, due to unknown effects by other components of magnetic perturbations. The offset is not possibly explained by other uncertainties such as unknown

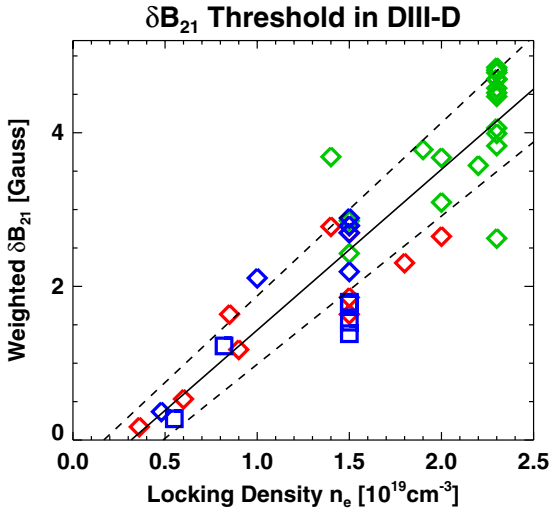

Figure 14. Correlations between the error field threshold and locking density using the total resonant fields. Locking cases described in this paper are all included: error field correction data for the left-handed (green) and right-handed (blue) plasmas. Error field correction data presented in [6] are in red. Approximately linear correlations are apparent as can be seen from the linear fit (solid) and its small standard deviation (dashed) of the fit. Note the offset of the linear scaling, which implies the importance of other contributions by the resonant field in other resonant surfaces or NTV effects.

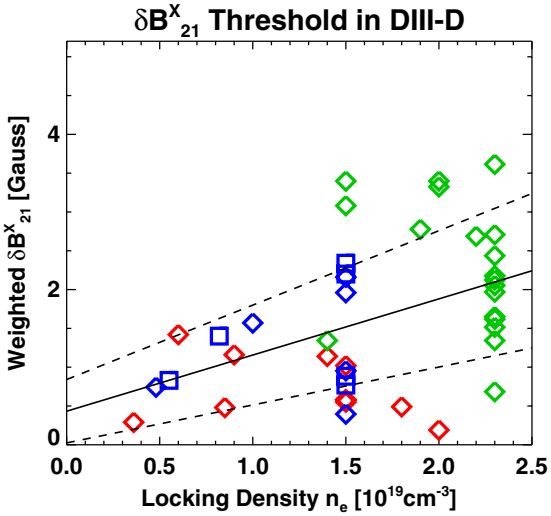

Figure 15. Correlations between the error field threshold and locking density using the external resonant fields. Locking cases described in this paper are all included: error field correction data for the left-handed (green) and right-handed (blue) plasmas. Error field correction data presented in [6] are in red. Correlations are very weak as can be seen from the large standard deviation (dashed) of the linear fit (solid).

intrinsic errors; as far as the only mode (such as δB_{21}) is concerned, the mode can be completely eliminated if a correction coil set can produce $n = 1$ with any fixed poloidal distribution and if $n = 1$ has a significant coupling to δB_{21}. Note that the empirically optimized correction is capable of eliminating one mode. Therefore, the offset implies that our choice of the critical field component alone, δB_{21}, is not sufficient and other contributions by the resonant field in other resonant surfaces or NTV effects may still be essential to achieve reliable predictability.

4. Theory—dominant external field and overlap

The total resonant field is the relevant physical quantity driving islands and locking as can be supported by the high correlation with plasma parameters such as density. However, what one actually can control in plasma operation is an external quantity, such as the external field—produced by currents in coils. The issue can be resolved if one can understand the coupling between the physically important plasma quantity and the external quantity. The *dominant external field* is introduced for this purpose. It is defined as the most important distribution of the external field to maximize the total resonant fields in the core, $\psi_N < 0.9$ [6, 25]. One can choose any control surface [26, 27], but the plasma boundary surface is a naturally convenient place to compute the external field.

The dominant external field is intuitive and can show where the fields should be applied to control the total resonant fields. One can approximately ignore other distributions since their contributions to the total resonant fields are weaker by an order of magnitude [25]. Then one can assume it is the only distribution to produce the total resonant fields and so one can define the *overlap* between the dominant external field and a given external field to measure the efficiency to drive the total resonant fields. The overlap is defined as

$$\mathcal{C} \equiv \oint d\varphi' \frac{\oint da(\delta \vec{B}^x \cdot \hat{n}_b)(\vartheta, \varphi' - \varphi)(\delta \vec{B}^x_d \cdot \hat{n}_b)(\vartheta, \varphi)}{\sqrt{\oint da(\delta \vec{B}^x \cdot \hat{n}_b)^2 \oint da(\delta \vec{B}^x_d \cdot \hat{n}_b)^2}}, \tag{1}$$

where (ϑ, φ) are magnetic angle coordinates, $\oint da$ is the surface integral, $(\delta \vec{B}^x \cdot \hat{n}_b)$ is the external field normal to the boundary surface and $(\delta \vec{B}^x_d \cdot \hat{n}_b)$ is the dominant external field normal to the boundary surface. If the given external field is equivalent to the dominant external field, then the overlap is 1, and it is 0 if the given external field is orthogonal to the dominant external field. The design of correction coils can be based on the dominant external field and the overlap. That is, the coils should produce an external field as close as possible to the dominant external field so that $\mathcal{C}$ approaches 1.

The overlap with the dominant external field explains precisely the variation of the efficiency dependence on the toroidal phasing, figure 8. Figure 16 shows the overlap between the external field with various toroidal phasings and the dominant external field. Both left and right configuration data are shown, but they are just mirror reflections of each other if one reverses the phasing (x-axis). It is not so difficult to notice their similarity to the inverse of figure 8. The worst phasing for the left-handed case (red in figure 16) is $\Delta\phi = 60°$, as one can see, the very large currents required in figure 8 are due to its poorest coupling in figure 16. If the overlap is close to 0, the required currents will increase indefinitely since $\mathcal{C} = 0$ means that the coils can never control the total resonant fields. The optimal phasing is $\Delta\phi = 240°$ (where 300° is almost good), as one can see the smallest required currents in figure 8 and the maximum overlap $\mathcal{C} \sim 0.65$. The overlap $\mathcal{C} \sim 0.32$

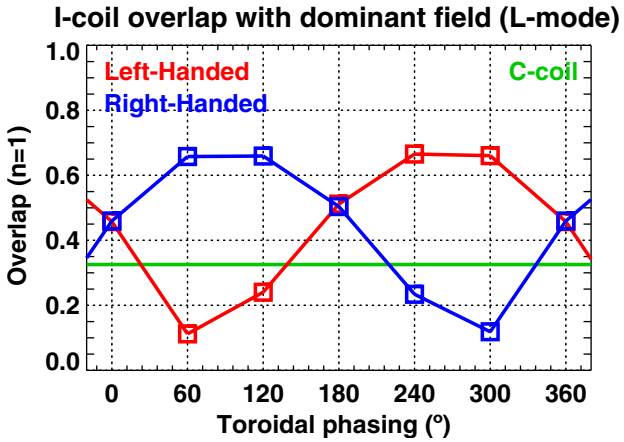

Figure 16. Overlap between the external field of I-coils and the dominant external field versus toroidal phasing between the upper and the lower I-coil arrays. The left-handed (red) and right-handed (blue) cases are shown, as well as the overlap of C-coils. One can see the similarity between the inverse of figure 8 and the red cases, indicating the relevance of the method using the dominant external field that is almost the only distribution driving the total resonant fields.

by DIII-D C-coils is also shown for comparison. Note that the dominant external field needs to be calculated by IPEC for only one representative of each family of Ohmic error field correction cases, since another great advantage of the dominant external field is that it is very robust across the plasma profiles and configurations [6, 25].

5. Summary

Various error field correction results in DIII-D Ohmic plasmas are presented. Optimal error field corrections using the two rows of I-coils are empirically established for their relative toroidal phasing, reference toroidal phase, and amplitude in coil currents, in both left-handed and right-handed plasmas. Various results can be explained far better based on error field threshold scaling by IPEC total resonant fields δB_{21} rather than vacuum external resonant fields δB^x_{21}. The efficiency of a correction coil configuration can also be well understood by the overlap between its external field and the dominant external field that is the most important distribution to drive the total resonant fields and plasma locking. However, the role of other components still needs to be understood, as can be highlighted by the offset of correlation when $\delta B_{21} \to 0$, to achieve reliable predictability in error field correction problems. Future work will include more comprehensive cross-machine parametric scaling using the total resonant fields, but should also address the issues with unknown components contributing to locking.

Acknowledgments

This work was supported by DOE contract DE-AC02-76CH03073 (PPPL) and DE-FC02-04ER54698 (GA).

References

[1] Hender T.C. *et al* 1992 *Nucl. Fusion* **32** 2091
[2] La Haye R.J., Fitzpatrick R., Hender T.C., Morris A.W., Scoville J.T. and Todd T.N. 1992 *Phys. Fluids* B **4** 2098
[3] Buttery R.J. *et al*, the JET Team, the COMPASS-D Research Team and the DIII-D Team 1999 *Nucl. Fusion* **39** 1827
[4] Scoville J.T. and La Haye R.J. 2003 *Nucl. Fusion* **43** 250
[5] Wolfe S.M. *et al* 2005 *Phys. Plasmas* **12** 056110
[6] Park J.-K., Schaffer M.J., Menard J.E. and Boozer A.H. 2007 *Phys. Rev. Lett.* **99** 195003
[7] Howell D.F., Hender T.C. and Cunningham G. 2007 *Nucl. Fusion* **47** 1336
[8] Menard J.E. *et al* and the NSTX Research Team 2010 *Nucl. Fusion* **50** 045008
[9] Fitzpatrick R. and Hender T.C. 1991 *Phys. Fluids* B **3** 644
[10] Fitzpatrick R. 1993 *Nucl. Fusion* **33** 1049
[11] Cole A. and Fitzpatrick R. 2006 *Phys. Plasmas* **13** 032503
[12] Shaing K.C. 2003 *Phys. Plasmas* **10** 1443
[13] Cole A., Hegna C.C. and Callen J.D. 2007 *Phys. Rev. Lett.* **99** 065001
[14] Park J.-K., Boozer A.H. and Menard J.E. 2009 *Phys. Rev. Lett.* **102** 065002
[15] Park J.-K., Boozer A.H. and Menard J.E. 2008 *Phys. Plasmas* **15** 064501
[16] Park J.-K., Boozer A.H., Menard J.E., Garofalo A.M., Schaffer M.J., Hawryluk R.J., Kaye S.M., Gerhardt S.P., Sabbagh S.A. and the NSTX team 2009 *Phys. Plasmas* **16** 056115
[17] Park J.-K., Boozer A.H. and Glasser A.H. 2007 *Phys. Plasmas* **14** 052110
[18] Luxon J.L. and Davis L.G. 1985 *Fusion Technol.* **8** 441
[19] Scoville J.T., La Haye R.J., Kellman A.G., Osborne T.H., Stambaugh R.D., Strait E.J. and Taylor T.S. 1991 *Nucl. Fusion* **31** 875
[20] La Haye R.J. and Scoville J.T. 1991 *Rev. Sci. Instrum.* **62** 2146
[21] Schaffer M.J., Menard J.E., Aldan M.P., Bialek J.M., Evans T.E. and Moyer R.A. 2008 *Nucl. Fusion* **48** 024004
[22] Jackson G.L. *et al* 2003 *Proc. 30th EPS Conf.* vol 27A (ECA) (*St Petersburg, Russia, 2003*) http://epsppd.epfl.ch/StPetersburg/PDF/P4_047.PDF
[23] Luxon J.L., Schaffer M.J., Jackson G.L., Leuer J.A., Nagy A., Scoville J.T. and Strait E.J. 2003 *Nucl. Fusion* **43** 1813
[24] Buttery R.J., Benedetti M.D., Hender T.C. and Tubbing B.J.D. 2000 *Nucl. Fusion* **40** 807
[25] Park J.-K., Boozer A.H., Menard J.E. and Schaffer M.J. 2008 *Nucl. Fusion* **48** 045006
[26] Boozer A.H. 1999 *Phys. Plasmas* **6** 3180
[27] Boozer A.H. 2003 *Phys. Plasmas* **10** 1458